

Generalization of exotic quark searches

F. Garberon, T. Golling

Yale University, New Haven CT, 06520, USA

General limits on exotic heavy quarks T , B and X with masses above 300 GeV are presented for arbitrary branching fractions of $T \rightarrow W^+b$, $T \rightarrow Zt$, $T \rightarrow Ht$, $B \rightarrow W^-t$, $B \rightarrow Zb$, $B \rightarrow Hb$ and $X \rightarrow W^+t$. The results are based on a CMS search in final states with three isolated leptons (e or μ) or two isolated leptons with the same electric charge. Exotic heavy quark pair production through the strong interaction is considered. In the context of vector-like quark models, T quarks with a mass $m_T < 480$ GeV and $m_T < 550$ GeV are excluded for weak isospin singlets and doublets, respectively, and B quarks with a mass $m_B < 480$ GeV are excluded for singlets, all at 95% confidence level. Mass limits at 95% confidence level for T and B singlets, (T,B) doublets and (X,T) doublets are presented as a function of the corresponding heavy quark masses. For equal mass $m_T = m_B$ and $m_X = m_T$ vector-like quarks are excluded at 95% confidence level with masses below 550 GeV for T and B singlets, 640 GeV for a (T,B) doublet and 640 GeV for a (X,T) doublet.

1. Introduction

Vector-like quarks [1, 2, 3] are new heavy quarks, in particular heavier than the top quark, which appear in many new physics models, such as extra dimensions, little Higgs, or composite Higgs models. Similar to a supersymmetric partner of the top quark, a vector-like top partner serves to stabilize the Higgs mass by cancelling the divergence of radiative corrections in the Higgs boson mass. Quarks are referred to as vector-like if their left- and right-handed chiralities transform in the same way under the electroweak group $SU(2) \times U(1)$. Vector-like quarks can be classified as weak isospin singlets, doublets or triplets. The mass eigenstates of these vector-like quarks are referred to as T and B , with charges $2/3$ and $-1/3$, respectively, and X and Y , with charges $5/3$ and $-4/3$, respectively. It is assumed that the new quarks mainly couple to the third generation [4] which leads to the following possible decay modes:

$$T \rightarrow W^+b, \quad T \rightarrow Zt, \quad T \rightarrow Ht,$$

$$B \rightarrow W^-t, \quad B \rightarrow Zb, \quad B \rightarrow Hb,$$

$$X \rightarrow W^+t,$$

$$Y \rightarrow W^-b.$$

For T and B singlets all decay modes are sizable. For doublets a reasonable assumption is that $V_{Tb} \ll V_{tB}$ so that only $T \rightarrow Zt$, $T \rightarrow Ht$ and $B \rightarrow W^-t$ contribute. In this paper we give special attention to this scenario but also present results that can be interpreted under more general CKM hypotheses. In addition, the branching fractions for the T and B decay modes vary with the heavy quark masses m_T and m_B , respectively. The total width of the new quarks is typically negligible as compared to the detector mass resolution in the probed mass range.

Exotic heavy quarks such as vector-like quarks are mainly produced in pairs through the strong interaction or singly via the electroweak interaction. We will only focus on the pair production. The cross section for this process is the same for each of these types of quarks and depends on the quark mass.

Using 4.9 fb^{-1} of pp collision data at $\sqrt{s} = 7$ TeV the CMS Collaboration excluded the existence of a fourth-generation b' quark with a mass below 611 GeV at 95% confidence level (CL) [5] by examining events with three isolated leptons (e or μ) or two isolated leptons with same electric charge. The ATLAS collaboration used a same-sign dilepton data sample equivalent to 4.7 fb^{-1} of pp collisions at $\sqrt{s} = 7$ TeV to exclude both b' and vector-like quarks

X with charge $5/3$ (which they referred to as $T_{5/3}$) with masses below 670 GeV at 95% CL [6]. A similar analysis was performed by the CMS Collaboration using 5 fb^{-1} of pp collisions at $\sqrt{s} = 7 \text{ TeV}$ to exclude vector-like quarks X with charge $5/3$ with masses below 645 GeV at 95% CL [7]. All three searches assume pair production through the strong interaction and branching ratios of unity $BR(b' \rightarrow W^- t) = 1$ and $BR(X \rightarrow W^+ t) = 1$.

However, same-sign-lepton or three-lepton signatures are expected from many of the vector-like-quark final states discussed above. Accounting for all possible decay processes, for $T\bar{T}$ production the possible final states are $W^+ b W^- b$, $W b Z t$, $W b H t$, $Z t Z t$, $Z t H t$ and $H t H t$. For $B\bar{B}$ production the possible final states are $W^- t W^+ t$, $W t Z b$, $W t H b$, $Z b Z b$, $Z b H b$ and $H b H b$. For $X\bar{X}$ production the only possible final state is $W^+ t W^- t$. For simplicity, here b represents both b and \bar{b} , and analogously for top quarks. Among these, all final states except $W^+ b W^- b$ feature same-sign-lepton or three-lepton signatures. In this paper we exploit this feature and reinterpret the published CMS result [5] by relaxing the assumptions which determine the branching ratios as a function of mass to explore the entire space of possible branching ratios. A similar reinterpretation for arbitrary branching fractions was performed by ATLAS [8] for an analysis targeting the $T\bar{T} \rightarrow W^+ b W^- b$ hypothesis in a single-lepton final state and excluding at 95% CL T quarks with a mass $400 \text{ GeV} < m_T < 500 \text{ GeV}$ for weak isospin singlets. We show that these limits can be extended with the same-sign-lepton and three-lepton signatures, and we present limits for the T and B singlet and doublet, as well as for the (X, T) doublet hypotheses as a function of the corresponding heavy quark masses. These represent important generalizations of the existing limits.

2. Samples and event selection

In this analysis the event selection of the CMS search is replicated as closely as possible. The selection is briefly described in Section 2.1. The details of how the selection is reproduced for this paper are discussed in Section 2.2.

2.1. The CMS event selection

As discussed above, CMS makes use of events that are selected under both same-sign and trilepton requirements (electron or muon). Events are selected if they pass a trigger that requires two leptons. Electrons are required to have $p_T > 20 \text{ GeV}$ and $|\eta| < 2.4$, excluding the region between the end-cap and barrel ($1.44 < |\eta| < 1.57$). Muons are required to have $p_T > 20 \text{ GeV}$ and $|\eta| < 2.4$. Jets are required to have $p_T > 25 \text{ GeV}$ and $|\eta| < 2.4$. For the same-sign analysis, CMS requires the presence of two isolated leptons with the same electric charge and at least four jets. For the trilepton analysis at least three isolated leptons must be identified, at least two of which must have an opposite charge, and at least two jets must be found. In all cases, at least one jet must be tagged as a b -jet using a tagger with roughly a 50% efficiency for identifying true b -jets, and events with two electrons or muons that are consistent with originating from a Z boson decay are rejected ($|m_{ll} - m_Z| > 10 \text{ GeV}$). Finally, the scalar sum of the transverse momenta of the jets, leptons, and the missing transverse momentum is required to be at least 500 GeV.

2.2. Samples and event selection for the reinterpretation

For this analysis samples of singlet $T\bar{T}$ and $B\bar{B}$ production, and doublet $X\bar{X}$ production were generated. All samples were generated using Protos 2.0 [1, 9] and showered using Pythia 6.4.25 [10]. 500,000 events were generated for each process and each mass hypothesis in 50 GeV intervals ranging from a lowest mass of 300 GeV to a highest mass of 900 GeV. In each case the Higgs mass was set to a value of 125 GeV.

The modeling of the CMS detector was performed using the Pretty Good Simulation (PGS) package [11], with the detailed detector descriptions taken from the default CMS detector card from the MadGraph [12] package. A few minor changes were then made to these defaults in order to improve the accuracy as discussed below. Some information, such as the CMS efficiencies for b -tagging and electron identification, is not provided in precise detail by the experiment. We document our assumptions below, and will show that we achieve good agreement with the published results.

All kinematic cuts on p_T and η of the leptons and jets are chosen to be identical to those of the experiment. PGS applies its own model for electron identification but it does not attempt to determine efficiency loss due to isolation cuts. In order to make the model more realistic we remove electrons if they are found to be within $\Delta R < 0.4$ of a jet with $p_T > 15$ GeV unless $\Delta R < 0.2$, in which case the jet is removed instead under the assumption that it is a misidentified electron. As the CMS documentation [13] does not give precise numbers for the selection efficiencies, we assume that their electrons have the same isolation efficiencies as for ATLAS [6]. The calorimeter and tracker cuts are each 90% efficient for the electron isolation at ATLAS.

Unlike for electrons, for muons PGS does not have a built-in muon identification model. Instead it only assumes a 2% inefficiency on all tracks in the analysis. This efficiency appears to be roughly correct for CMS, which has highly efficient muon selection and isolation requirements [14].

CMS has triggers that are highly efficient for electron identification, but less efficient for muon identification. CMS explicitly quotes their trigger efficiencies for their selected events as being 91% in the $\mu\mu$ channel, 96% in the $e\mu$ channel, and 99% in the ee channel [5]. When simulating the same-sign dilepton analysis for CMS, events are randomly thrown out according to these probabilities. For the CMS trilepton analysis the triggers are assumed to be 100% efficient.

The b -tagging efficiency for state-of-the-art CMS b -tagging algorithms is quite different from the efficiency that is assumed by PGS. We therefore set the b -tagging efficiency to more appropriate values. For CMS a tagger was chosen that was tuned to be 50% efficient for real b -jets with a 1% mistagging efficiency for non- b jets [5]. In principle it would be best to account for the p_T and η -dependence of the tagging efficiencies. Unfortunately, none of the CMS public b -tagging documents [15, 16] provide the efficiencies of this particular operating point as a function of jet kinematics. This documentation does, however, indicate that the b -taggers in CMS tend to have less kinematic dependence than at many other experiments. We therefore instead use the average efficiency of 50% for real b -jets and 1% for non- b jets as quoted in the paper [5].

After applying all event selection, the PGS event yields are validated against the quoted CMS yields for the pair production of b' quarks. As shown in the ATLAS analysis [6], these yields are approximately identical to the X pair production yields. For purposes of this validation, since CMS assumes $BR(b' \rightarrow W^- t) = 1$ [5, 6, 7], we apply a filter to force the vector-like-quarks to decay in the same manner ($BR(B \rightarrow W^- t) = 1$). Very good agreement is found as shown in Table I.

	$m_{b'/B} = 450$ GeV	$m_{b'/B} = 500$ GeV	$m_{b'/B} = 550$ GeV	$m_{b'/B} = 600$ GeV	$m_{b'/B} = 650$ GeV
PGS same-sign	49.9 ± 1.4	25.1 ± 0.7	14 ± 0.4	7.9 ± 0.2	4.1 ± 0.1
CMS same-sign	49 ± 4.2	26 ± 2.2	14 ± 1.1	7.6 ± 0.6	4.3 ± 0.4
CMS SS Difference (%)	1.8 ± 9	-3.4 ± 8.9	0 ± 8.6	3.7 ± 8.7	-4.1 ± 9.1
PGS trilepton	16 ± 0.8	8.1 ± 0.4	4.5 ± 0.2	2.6 ± 0.1	1.5 ± 0.1
CMS trilepton	15 ± 1.6	8.2 ± 0.8	4.7 ± 0.4	2.7 ± 0.3	1.6 ± 0.2
CMS trilepton Difference (%)	6.6 ± 11.9	-0.6 ± 10.9	-3.5 ± 9.9	-5.3 ± 10.8	-8.3 ± 10.2

Table I: Comparison of the number of expected signal events passing all selection requirements between PGS and the quoted results from the CMS paper for both the same-sign and the trilepton selections, normalized to the CMS integrated luminosity of 4.9 fb^{-1} . Uncertainties on the CMS paper results include both statistical and systematic uncertainties, while uncertainties on the PGS result are statistical only.

3. Method

This analysis proceeds in three steps. First, events are selected according to the prescriptions documented in Section 2. It must be remembered that in the case of $B\bar{B}$ and $T\bar{T}$ events, the simulation assumes that the heavy quarks are singlets. When predictions for a model with alternate decays such as a doublet model are desired instead,

a correction is needed to the appropriate decay branching fractions. This procedure is described in Section 3.1. Finally, the number of observed events is converted into exclusion limits. This procedure is discussed in Section 3.2.

3.1. Alternate decay-mode hypotheses

Depending on how each of the new heavy quarks decays, there are six possible combinations for each quark type as explained in Section 1. The nominal $T\bar{T}$ and $B\bar{B}$ samples in this analysis are generated with the hypothesized branching fractions for the new heavy quark decays that is appropriate for singlets. In this section we explain how the expected number of signal events is converted to a value that is appropriate to more general branching fractions such as under a doublet model.

To achieve full generality, for each mass point a two dimensional grid of all possible branching fractions is scanned in 10% steps. The dimensions are chosen to be the branching ratio of the W -type decay modes, which we denote B_W , and the branching ratio of the Z -type decay modes, which we denote B_Z . The branching ratio of the Higgs-type decays follows from $B_H = 1 - B_W - B_Z$. The probability for the production of each of the six possible combinations of decays of the two new heavy quarks then depends upon these branching fractions that we are assuming. For a particular decay mode i , the probability is denoted $P_i(B_W, B_Z)$. After determining the acceptance times efficiency for our event selection for each decay, A_i , the number of signal events N that is expected for each hypothesis branching fraction is then determined according to Equation 1:

$$N = \sum_{i=1}^6 P_i(B_W, B_Z) A_i \int \mathcal{L} \sigma, \quad (1)$$

where $\int \mathcal{L}$ is the integrated luminosity and σ is the corresponding heavy quark pair production cross section. We assume that the kinematic differences and consequently the differences in selection efficiency for singlets and doublets are negligible.

3.2. Limit setting

In order to set limits on a given model it is necessary to know the following information for each measurement: the number of expected background events from each source with their associated uncertainties, the number of expected signal events with their associated uncertainty, and the number of observed data events.

The number of data events, the number of background events from each source, and their respective uncertainties are taken directly from the CMS paper. The predictions for the signal model are taken from the outputs of the PGS simulation, with any necessary corrections applied as discussed in Sections 2.2 and 3.1 to arrive at a given decay hypothesis. In all cases, systematic uncertainties on the signal are assumed to have the same relative size as are quoted in the paper.

Generally it is necessary to split the uncertainties for each sample into their components in order to correctly handle correlations between the signal and background samples. However, in all cases considered here, the systematic uncertainties that are correlated between samples are negligibly small and can be safely neglected. In particular, for the same-sign analysis the dominant background systematics are due to control-region estimations, which are not correlated to the signal uncertainties. Similarly, in the trilepton analysis the dominant background uncertainties are from data statistics, normalization of the theoretical backgrounds, and Monte Carlo sample statistics, which again are not correlated to the signal uncertainties. We therefore neglect correlations when running the limit-setting. In tests we were able to reproduce the limit results for the CMS results (and for the similar ATLAS results [6]) to within 10 GeV in mass under this assumption.

Limit setting is performed by running the MCLimit [17, 18] program simultaneously on the same-sign and the trilepton results. In order for the limit setting to converge with high accuracy, tens (or hundreds) of thousands of pseudo-experiments must be performed for each signal hypothesis. When scanning over all of the mass and

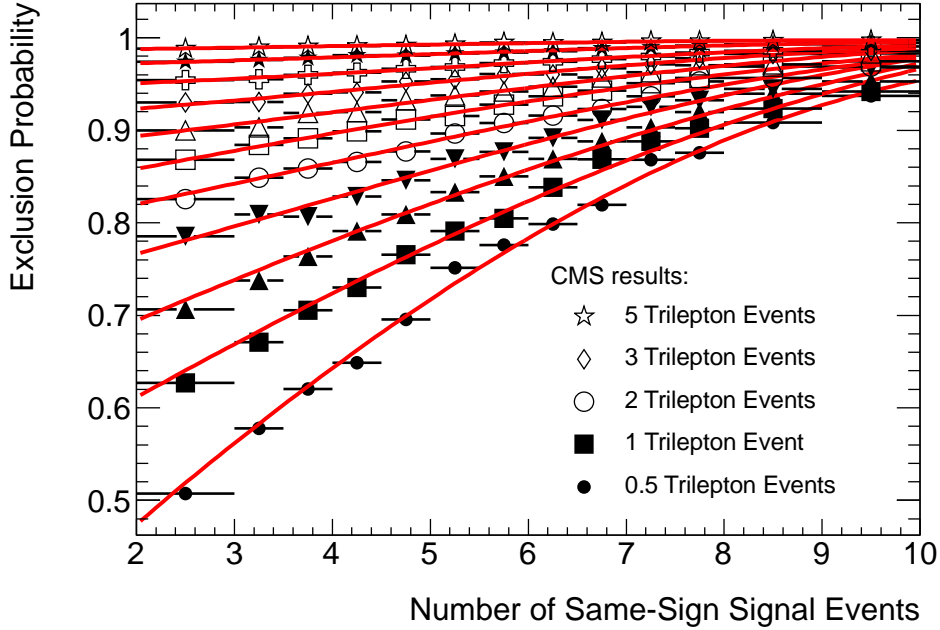


Figure 1: The expected exclusion probabilities as a function of the number of expected signal events are plotted. A two-dimensional parametrization is needed in the predicted number of same-sign and trilepton events. The x -axis shows the number of same-sign signal events, while fit functions are overlaid depending on the number of trilepton signal events. Eleven functions are shown for bins of between 0.5 and 6.0 trilepton events, representing bins with the following bounds: $\{0.5, 1.0, 1.33, 1.67, 2.0, 2.33, 2.67, 3.0, 3.5, 4.0, 5.0, 6.0\}$. The goal is to determine where each parametrization crosses the 95% threshold exclusion probability. A linear interpolation is applied to determine the proper functional form for the number of trilepton events in between bin centers.

branching-fraction parameters that are considered for the signal models in this paper this procedure becomes very computationally intensive. A simplification is therefore made in order to streamline the process. Since results of the limit setting will depend only on the predicted signal yields for each model, the exclusion probability can therefore be parametrized in two variables: the number of predicted same-sign and trilepton signal events. These variables are scanned and MCLimit predictions are made at periodic steps. Functions are fit to interpolate and smooth the results between these points. Results are shown in Figure 1.

4. Results

In Section 4.1 the results of the analysis assuming arbitrary branching fractions for heavy quark $T\bar{T}$ and $B\bar{B}$ decays are presented. In Section 4.2 these results are interpreted in the context of certain theoretically motivated values of heavy quark branching fractions, including the (X, T) doublet.

4.1. Results for arbitrary branching fractions for the new heavy quark decays

In this section results are presented for all possible branching fractions of heavy T and B quark decays. In each case we assume only the presence of a single $T\bar{T}$ or $B\bar{B}$ production process. Having both $T\bar{T}$ or $B\bar{B}$ present would of course lead to improved sensitivity. We discuss some such models with two new heavy quarks later in Section 4.2.

After selecting events from the signal samples that pass the selection requirements, the number of expected events as a function of the branching ratio of the decays of the new heavy quarks are determined according to the prescription

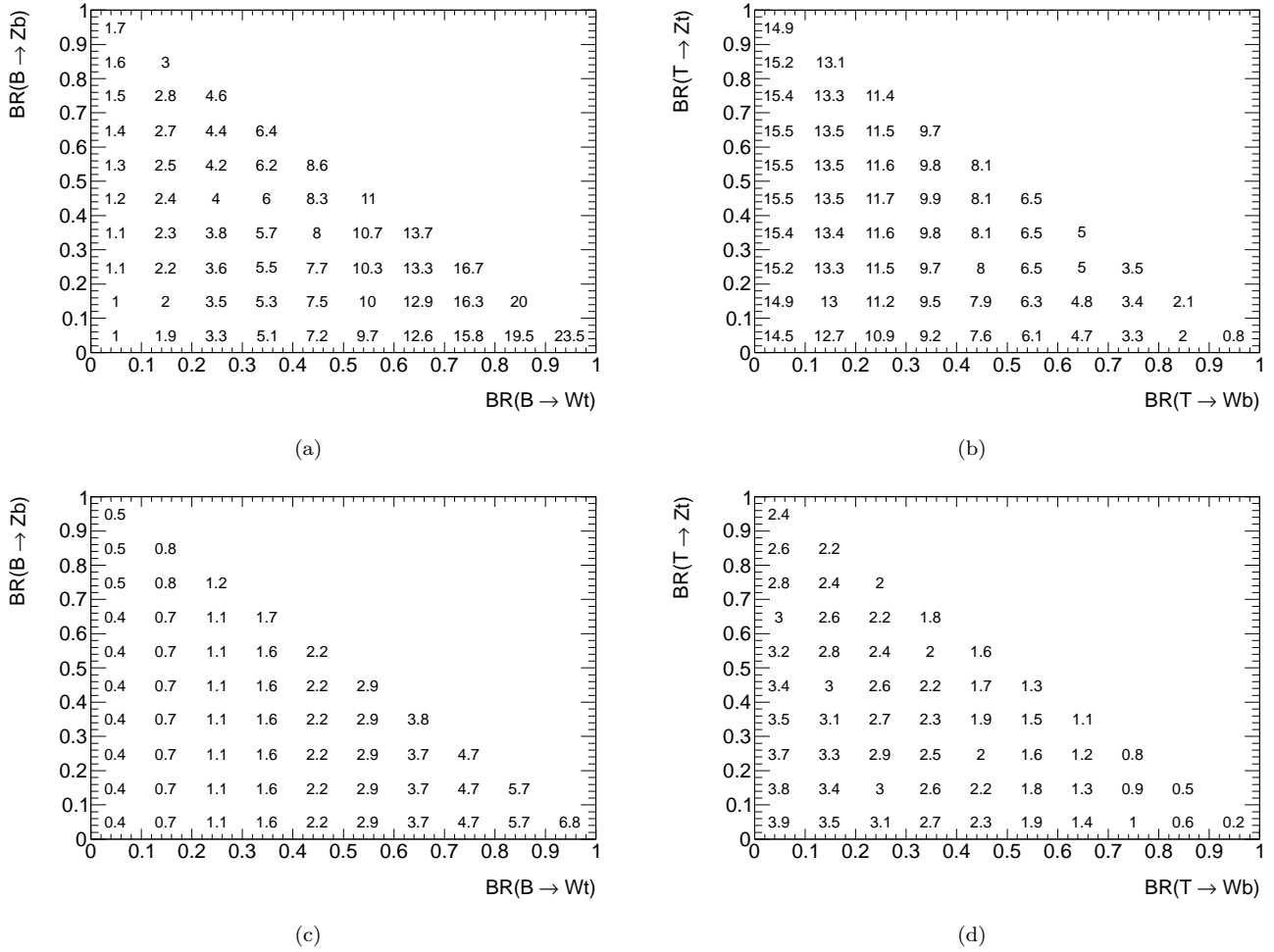


Figure 2: Here we show the number of expected signal events depending on the model for pair production of quarks with a mass of 500 GeV: same-sign yields for $B\bar{B}$ (a) and $T\bar{T}$ (b) production, and trilepton yields for $B\bar{B}$ (c) and $T\bar{T}$ (d) production.

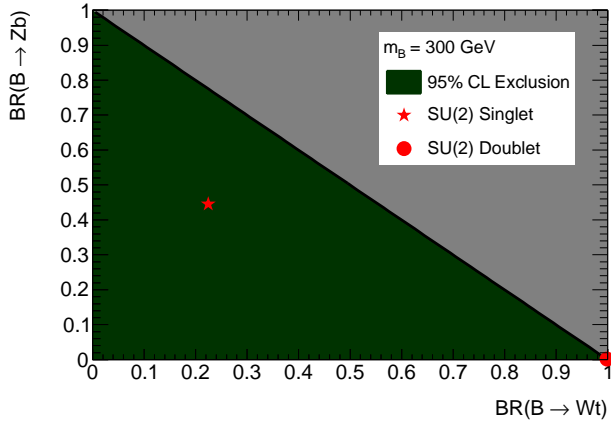
of Section 3.1. These numbers are shown for example production processes in Figure 2. In each case the number of events are then interpreted as an exclusion limit according to the parameterizations of Figure 1.

The resulting exclusion values are shown in Figures 3 and 4 for the possible signal hypotheses. At 95% CL we exclude T quarks with a mass $m_T < 480$ GeV and $m_T < 550$ GeV for weak isospin singlets and doublets, respectively and B quarks with a mass $m_B < 480$ GeV for singlets. These doublet-limits are quoted assuming $V_{Tb} \ll V_{tB}$. Production of $B\bar{B}$ and $T\bar{T}$ are both excluded at 95% CL for all possible branching ratios up to a mass of 360 GeV. When considering the results of the ATLAS search [8] in addition to those of this paper, the $T\bar{T}$ hypothesis is excluded for all branching ratios up to a mass of 450 GeV.

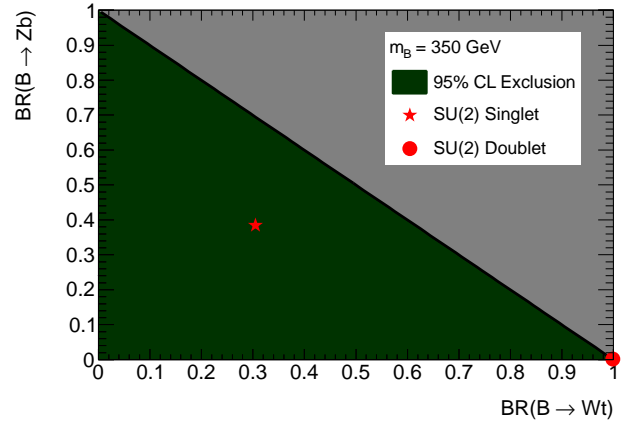
4.2. Results assuming nominal branching fractions for the new heavy quark decays

In this section results are presented under certain plausible models. After determining the number of events that are expected to pass selection for each signal hypothesis, the results are interpreted as exclusion limits according to the parameterizations of Figure 1.

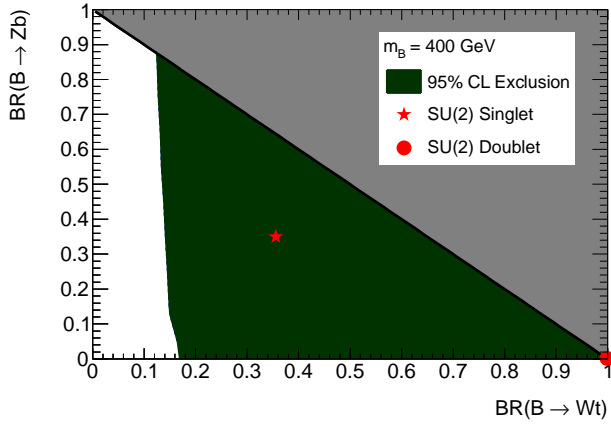
The first hypothesis is that both a B and a T singlet are present with the expected branching ratios. In this case the default Protos model has the correct branching fractions and no corrections are required. Alternately, we consider the presence of a (B, T) (with $V_{Tb} \ll V_{tB}$) or a (X, T) doublet. For each of these models, the limit results



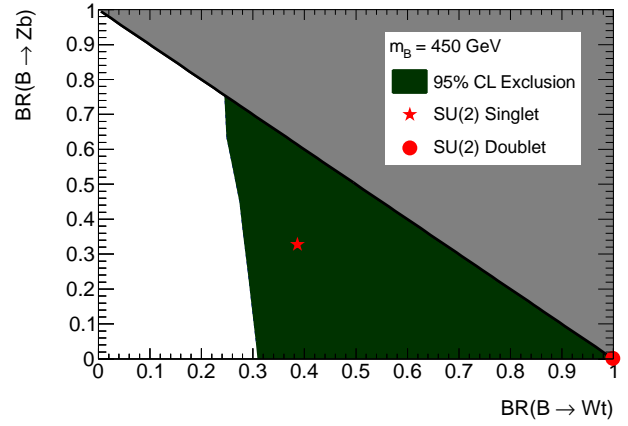
(a)



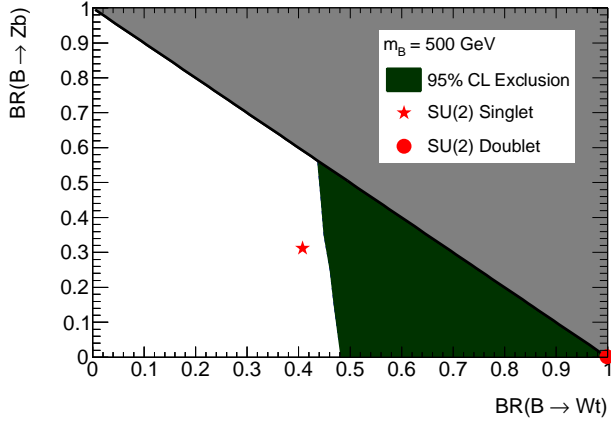
(b)



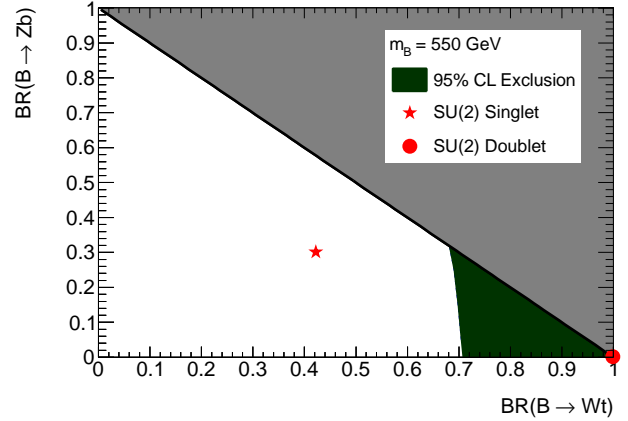
(c)



(d)

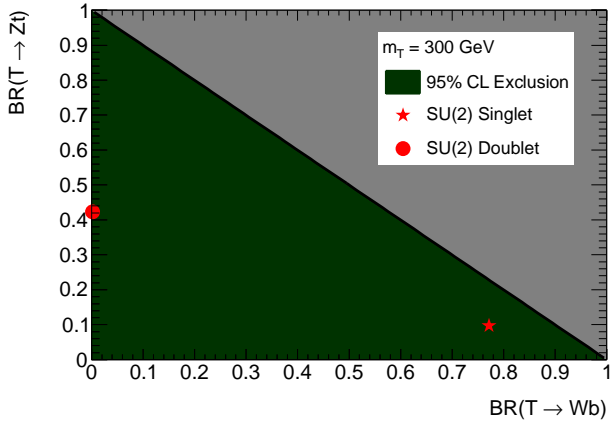


(e)

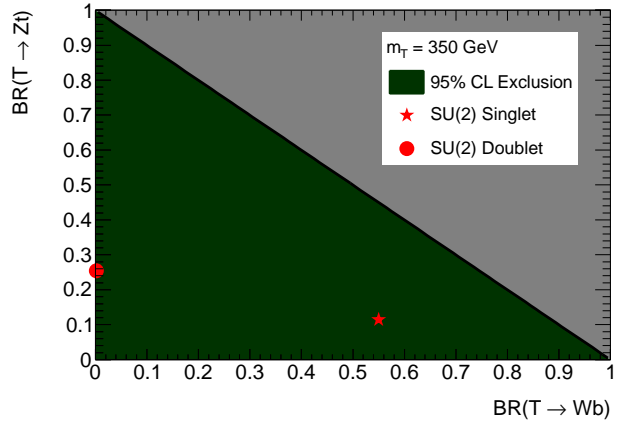


(f)

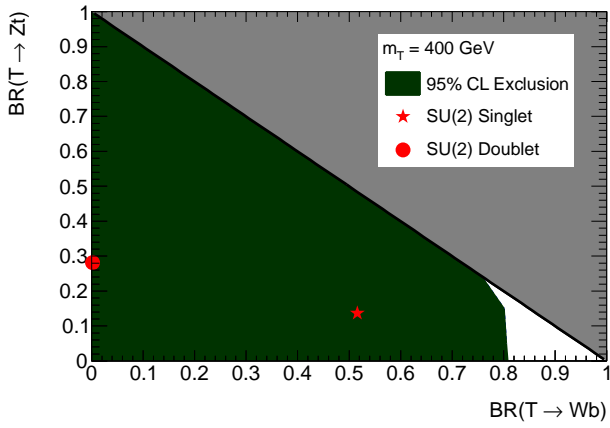
Figure 3: Here we show the 95% CL exclusion regions for $B\bar{B}$ pair production depending on the assumed branching ratios. The actual branching fractions depend on the parameters of the model. In each case the branching fractions of the singlet model are indicated by a star. For the doublet model, the branching ratios depend on the CKM parameters. Branching fractions under the reasonable scenario of $V_{Tb} \ll V_{tB}$ are shown as a circle. Results are shown assuming a B mass of 300 GeV (a), 350 GeV (b), 400 GeV. (c), 450 GeV (d), 500 GeV (e) and 550 GeV (f).



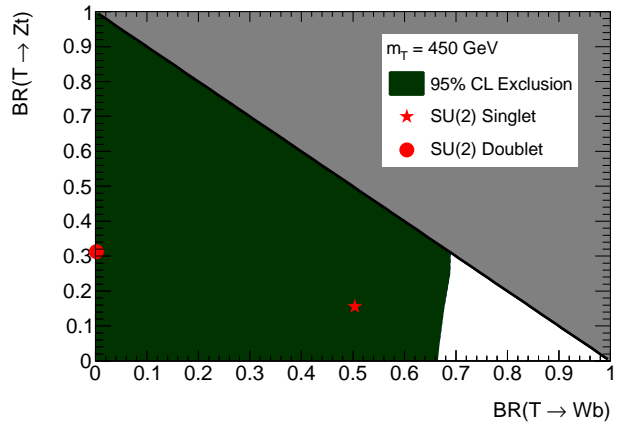
(a)



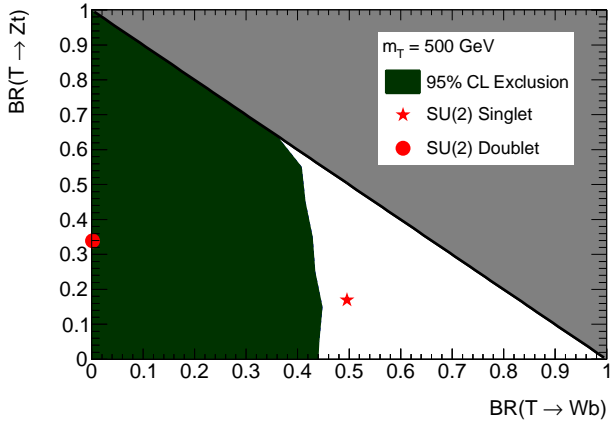
(b)



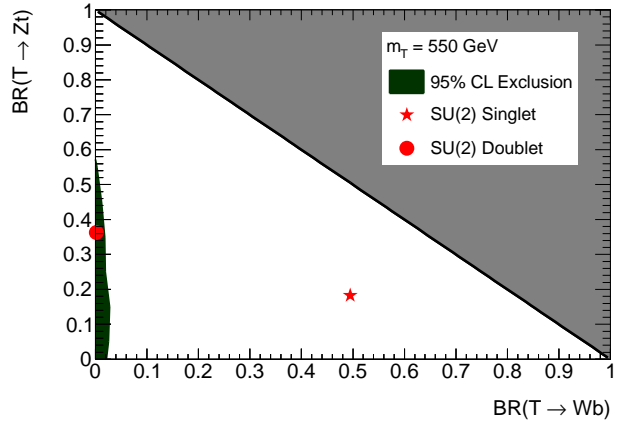
(c)



(d)



(e)



(f)

Figure 4: Here we show the 95% CL exclusion regions for $T\bar{T}$ pair production depending on the assumed branching ratios. The actual branching fractions depend on the parameters of the model. In each case the branching fractions of the singlet model are indicated by a star. For the doublet model, the branching ratios depend on the CKM parameters. Branching fractions under the reasonable scenario of $V_{Tb} \ll V_{tB}$ are shown as a circle. Results are shown assuming a T mass of 300 GeV (a), 350 GeV (b), 400 GeV. (c), 450 GeV (d), 500 GeV (e) and 550 GeV (f).

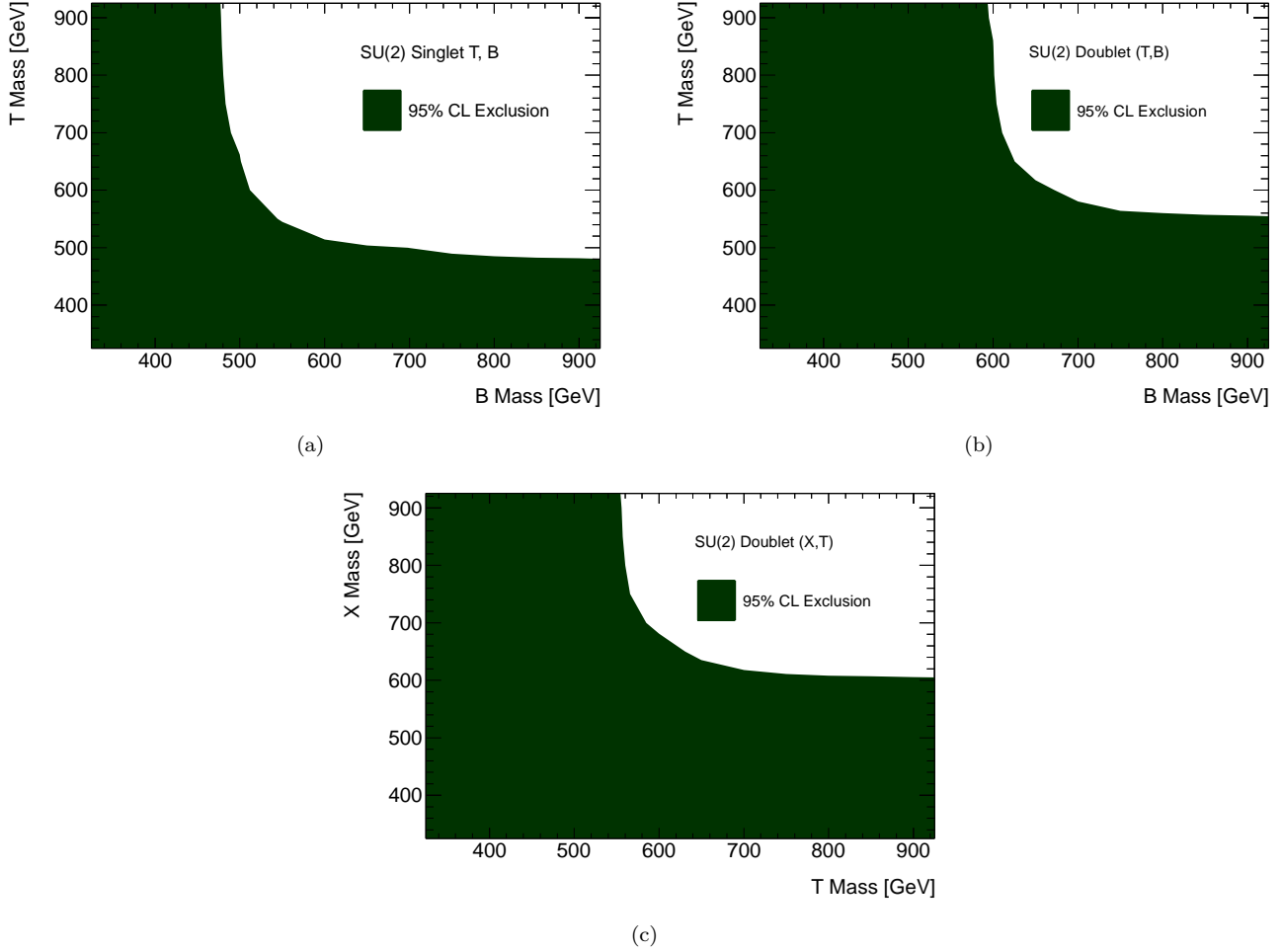


Figure 5: Here 95% CL exclusion limits are shown depending on the mass of each quark and the model. Figure (a) shows results assuming the presence of two singlets, T and B . Figure (b) shows results assuming the presence of a (T, B) doublet under the assumption $V_{Tb} \ll V_{tB}$. Figure (c) shows results assuming the presence of a (X, T) doublet.

are presented in Figure 5 in a two-dimensional grid depending on the hypothesized mass of the new heavy quarks. It should be noted that in the case of the singlet model there is no reason to assume that both a B and a T quark must be present. In case only a single quark is present, the limits can be extracted by considering the high-mass limit for the other quark in Figure 5.

Assuming identical masses for the new heavy quarks in the singlets and doublets, the 95% CL limits can be interpreted as $m_Q < 550$ GeV for the case of a singlet T and a singlet B , $m_Q < 640$ GeV for the case of a doublet (T, B) , and $m_Q < 640$ GeV for the case of a doublet (X, T) .

5. Conclusion

We demonstrate in this paper that searches in final states with three isolated leptons (e or μ) or two isolated leptons with same electric charge have a very good sensitivity to exotic heavy quarks T , B and X for all possible decay modes $T \rightarrow W^+b$, $T \rightarrow Zt$, $T \rightarrow Ht$, $B \rightarrow W^-t$, $B \rightarrow Zb$, $B \rightarrow Hb$ and $X \rightarrow W^+t$. ATLAS and CMS searches in these final states have previously set limits assuming $BR(b' \rightarrow W^-t) = 1$ and $BR(X \rightarrow W^+t) = 1$. We reinterpret CMS results and generalize their limits for arbitrary branching ratios for heavy quark masses above 300 GeV.

For vector-like quark models we exclude at 95% CL T quarks with a mass $m_T < 480$ GeV and $m_T < 550$ GeV for

weak isospin singlets and doublets, respectively and B quarks with a mass $m_B < 480$ GeV for singlets. Mass limits at 95% CL for T and B singlets, (T, B) doublets and (X, T) doublets are presented as a function of the corresponding heavy quark masses. Under an equal mass hypothesis ($m_T = m_B$ and $m_X = m_T$) vector-like quarks are excluded at 95% CL with masses below 550 GeV for T and B singlets, 640 GeV for (T, B) doublets (assuming $V_{Tb} \ll V_{tB}$) and 640 GeV for (X, T) doublets.

6. Acknowledgements

We thank Juan Antonio Aguilar-Saavedra and Nuno Castro for useful comments. The authors are supported by grants from the Department of Energy Office of Science and by the Alfred P. Sloan Foundation.

References

- [1] J. A. Aguilar-Saavedra, “Identifying top partners at LHC,” *JHEP*, vol. 0911, p. 030, 2009.
- [2] J. A. Aguilar-Saavedra, “Pair production of heavy singlets at LHC,” *Physics Letters B*, vol. 625, no. 3-4, pp. 234–244, 2005.
- [3] F. del Aguila, J. Santiago, and M. Pérez-Victoria, “Observable contributions of new exotic quarks to quark mixing,” *JHEP*, vol. 0009, p. 010, 2000.
- [4] F. del Aguila and M. J. Bowick, “The possibility of new fermions with $\Delta I = 0$ mass,” *Nucl. Phys.*, vol. B224, p. 107, 1983.
- [5] CMS Collaboration, “Search for heavy bottom-like quarks in 4.9 inverse femtobarns of pp collisions at $\sqrt{s} = 7$ TeV,” *JHEP*, vol. 1205, p. 123, 2012.
- [6] ATLAS Collaboration, “Search for exotic same-sign dilepton signatures (b' quark, $T_{5/3}$ and four top quarks production) in 4.7 fb⁻¹ of pp collisions at $\sqrt{s} = 7$ TeV with the ATLAS detector,” ATLAS-CONF-2012-130, 2012.
- [7] CMS Collaboration, “Search for a heavy partner of the top quark with charge 5/3,” CMS-PAS-B2G-12-003, 2012.
- [8] ATLAS Collaboration, “Search for pair production of heavy top-like quarks decaying to a high-pT W boson and a b quark in the lepton plus jets final state at $\sqrt{s} = 7$ TeV with the ATLAS detector,” *Physics Letters B*, vol. 718, no. 4-5, pp. 1284–1302, 2013.
- [9] J. A. Aguilar-Saavedra, “PROTOS, A Program for Top Simulations,” <http://jaguilar.web.cern.ch/jaguilar/protos/>, 2009.
- [10] T. Sjostrand, S. Mrenna, and P. Z. Skands, “PYTHIA 6.4 Physics and Manual,” *JHEP*, vol. 0605, p. 026, 2006.
- [11] J. Conway, <http://www.physics.ucdavis.edu/~conway/research/software/pgs/pgs.html>.
- [12] J. Alwall, M. Herquet, F. Maltoni, O. Mattelaer, and T. Stelzer, “MadGraph 5 : Going Beyond,” *JHEP*, vol. 1106, p. 128, 2011.
- [13] CMS Collaboration, “Electron reconstruction and identification at $\sqrt{s} = 7$ TeV,” CMS-PAS-EGM-10-004, 2010.
- [14] CMS Collaboration, “Performance of CMS muon reconstruction in pp collision events at $\sqrt{s} = 7$ TeV,” *JINST*, vol. 7, p. P10002, 2012.
- [15] CMS Collaboration, “Identification of b -quark jets with the CMS experiment,” 2012. arXiv:hep-ex/1211.4462.
- [16] CMS Collaboration, “Measurement of b -tagging efficiency using $t\bar{t}$ events,” CMS-PAS-BTV-11-003, 2012.
- [17] T. Junk, “Confidence level computation for combining searches with small statistics,” *Nucl. Instrum. Meth.*, vol. A434, pp. 435–443, 1999.
- [18] A. L. Read, “Presentation of search results: the CLs technique,” *Journal of Physics G: Nuclear and Particle Physics*, vol. 28, no. 10, pp. 2693–2704, 2002.